



Original Research Article

Assessing bioactivity of environmental water samples filtered using nanomembrane technology and mammalian cell lines

Sarah E. Morgan^{a,d}, Lisa A. DeLouise^{a,b,c,d,*}^a Department of Environmental Medicine, University of Rochester Medical Center, Rochester, NY 14642, USA^b Department of Biomedical Engineering, University of Rochester, Rochester, NY 14627, USA^c Department of Dermatology, University of Rochester Medical Center, Rochester, NY 14642, USA^d Lake Ontario Center for Microplastics and Human Health in a Changing Environment, University of Rochester Medical Center, Rochester, NY 14642, USA

ARTICLE INFO

Keywords:

Microplastics

SiN nanomembranes

Lake Ontario

Aryl hydrocarbon receptor (AhR) activity

IL-6 levels

Bioactivity

ABSTRACT

This project reports on the use of a novel nanomembrane filtering technology to isolate and analyze the bioactivity of microplastic (MP)-containing debris from Lake Ontario water samples. Environmental MPs are a complex mixture of polymers and sorbed chemicals that are persistent and can exhibit a wide range of toxic effects. Since human exposure to MPs is unavoidable, it is necessary to characterize their bioactivity to assess potential health risks. This work seeks to quantify MP presence in the nearshore waters of Lake Ontario and begin to characterize the bioactivity of the filtrate containing MPs. We utilized silicon nitride (SiN) nanomembrane technology to isolate debris sized between 8 and 20 μm from lake water samples collected at various times and locations. MPs were identified with Nile red staining. Cell-based assays were conducted directly on the filtered debris to test for cell viability, aryl hydrocarbon receptor (AhR) activity, and interleukin 6 (IL-6) levels as a measure of proinflammatory response. All samples contained MPs. None of the isolated debris impacted cell viability. However, AhR activity and IL-6 levels varied over time. Additionally, no associations were observed between the amount of plastic and bioactivity. Observed differences in activity are likely due to variations in the physicochemical properties of debris between samples. Our results highlight the need for increased sampling to fully characterize the bioactivity of MPs in human cells and to elucidate the role that sample physicochemical and spatiotemporal properties play in this activity.

1. Introduction

Plastic pollution is a major problem worldwide, with over ten million tons entering the environment annually [1]. A large portion of this plastic pollution can be characterized as microplastics (MPs) or nanoplastics (NPs). MPs are small pieces of plastic that range in size from 1 μm to 5 mm [2,3]. There are two types of MPs: primary and secondary. Primary MPs are particles that are manufactured at the micro-size level and in pre-production pellets and microbeads in consumer products [4]. On the other hand, secondary MPs are produced by the degradation of larger plastic debris in the environment [5,6]. Once these particles fall below 1 μm in size, they are classified as NPs [7,8]. Although plastics degrade in the environment, they are estimated to persist for hundreds of years [9] and thus comprise a ubiquitous environmental contaminant. MPs have been detected on all seven continents [10] and in various geographical features including oceans [11], lakes [12], rivers [13], soil [14], and air

[15]. Proximity to urban areas has been positively linked with an increased presence of plastic particles [16]. Researchers have detected both spatial and temporal variations within samples from the same water source [17,18]. Temporal trends varied as some studies found no clear trend [19], whereas others observed an increase in MPs over time [20]. Investigating temporal trends through a seasonal lens may not provide sufficient information for establishing conclusive trends. Depending on the study, MP contamination is higher in either the wet [21] or the dry [22] seasons. MPs are widespread but are differentially impacted by various environmental factors.

In addition to being a ubiquitous environmental contaminant, MPs have been found in various foodstuffs, including honey [23], sugar [23], bottled water [24,25], and milk [26]. Given the persistent nature and ubiquity of plastic, human exposure to MPs is inevitable. Therefore, it is important to characterize the risks to human health associated with this exposure. This is especially challenging, given that a key characteristic of

* Corresponding author.

E-mail address: lisa_delouise@urmc.rochester.edu (L.A. DeLouise).<https://doi.org/10.1016/j.eehl.2024.05.004>

Received 23 February 2024; Received in revised form 10 May 2024; Accepted 21 May 2024

Available online 29 May 2024

2772-9850/© 2024 The Author(s). Published by Elsevier B.V. on behalf of Nanjing Institute of Environmental Sciences, Ministry of Ecology and Environment (MEE) & Nanjing University. This is an open access article under the CC BY-NC-ND license (<http://creativecommons.org/licenses/by-nc-nd/4.0/>).

environmental MPs is their high degree of heterogeneity due to a wide range of polymers, adsorbed pollutants, morphologies, and dimensions present [27]. The sorbed chemicals include both those added during production to alter the plastic's properties to suit their post-production use [28] and contaminants picked up after plastic enters the environment [29]. Contaminants that have been identified in MP samples include plasticizers such as bisphenol A (BPA), an endocrine-disrupting chemical (EDC), polychlorinated biphenyls [30,31], aryl hydrocarbon receptor (AhR) agonists [32], and heavy metals [33]. Due to the widespread presence of MPs and the vast pool of AhR and EDC ligands, it is highly likely that most environmental MPs contain these chemical classes. The AhR is a promiscuous receptor that is considered to be a xenobiotic sensor [34]. It is of particular interest since exogenous activation is associated with disruptions to homeostasis and immunity and with increased cancer susceptibility [35]. Additionally, MPs may act similarly to other particulate matter exposures to induce inflammation. One broad measure of inflammation in cells is interleukin 6 (IL-6) levels [36]. Previous studies have investigated these endpoints in pure MPs [37–39]. Therefore, AhR activity and IL-6 concentration are putative measures of bioactivity worth studying in environmental samples.

This study seeks to investigate the bioactivity of environmental debris sourced from the nearshore waters of Lake Ontario (LO). LO is the largest body of water in Western New York. The LO water basin serves approximately 9 million people between the United States and Canada [40]. Residents rely on the lake for freshwater access, including drinking water, fishing, and recreational activities such as swimming and boating. Different areas of the LO shoreline are used for different activities depending on factors such as the availability of sandy beachfront access, surface current, and pollutant levels related to proximity to rivers and tributaries. Potential seasonal trends are of interest in relation to LO, as there is an increase in water entering the lake following snow thawing in the spring that could alter the MPs in the lake. Additionally, lake usage by residents is season-dependent; therefore, understanding whether exposure risk and/or hazard varies between seasons would be important for the development of guidelines for minimizing exposure impact. One common limitation with environmental samples is that it is difficult to isolate particles at the lower end of the MP size range [41] and nearly impossible to isolate NPs [42]. To overcome this limitation, we utilized commercial nanomembrane filters to isolate particles sized between 8 and 20 μm . The nanomembranes have additional benefits, including being biologically inert, optically clear, plastic-free, resistant to clogging, and having a faster flow rate than other filters [43,44]. In addition to the novelty of the size range, smaller MPs were targeted because laboratory studies have shown smaller particles are more toxic [45,46].

In this study, water samples were collected from four lakeshore locations at up to four timepoints across multiple years. Environmental debris was isolated using nanomembrane filters, and plastic presence was confirmed via Nile red staining. Bioactivity was measured using assays for AhR activity and IL-6 levels. Our results suggest that the innovative method for isolating smaller MPs from water samples described has applications for future samples while highlighting the need for a better understanding of the impacts of sample physical/chemical, spatial, and temporal properties on MP bioactivity and the risk these particles pose to human health. Developing methods to sample plastics in the nanoparticle size range is also critical for assessing human health impacts.

2. Methods

2.1. Sample collection

Up to five 1-L water samples were collected from the nearshore waters of LO (approximately 6 inches beneath the surface of water, approximately 2 feet deep) from up to four locations (Fig. 1). Samples were collected from Ontario Beach Park (OBP) (location 2) on November 10, 2021, July 19, 2022, February 17, 2023, and April 21, 2023. On April 21, 2023, samples were also collected from Hamlin Beach (HB) (location

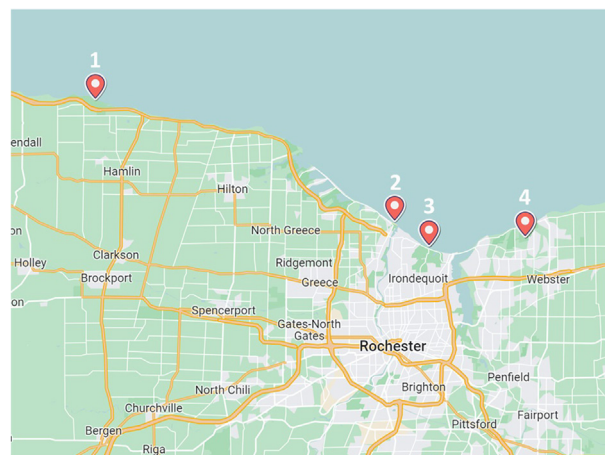


Fig. 1. Map of sampling locations. Water samples were collected from Lake Ontario at (1) Hamlin Beach State Park (HB), (2) Ontario Beach Park (OBP), (3) Durand Eastman Beach (DEB), and (4) Webster Park (WP). Created with Proxi.

1), Durand Eastman Beach (DEB) (location 3), and Webster Park (WP) (location 4). Locations were selected due to the variety of uses of the beaches and surrounding land. Visitors are attracted to Hamlin Beach State Park for its clear water and sandy beaches [47]. Similarly, OBP has a beach and water access, but the water is less attractive due to the proximity of the mouth of the polluted Genesee River, so there is less swimming, but the proximity to the city of Rochester translates to plenty of boating [48]. DEB is similarly near the city, but due to strong currents, there are limited swimming hours [49]. Lastly, WP has a rocky beach and pier, so activities there mainly include fishing [50]. Clean 1-L glass bottles were rinsed three times in lake water before being filled and capped underwater. The bactericide sodium azide (0.05%) was added to the samples to prevent growth. Prior to collection, bottles were scrubbed with soap, rinsed three times with tap water, rinsed three times with deionized (DI) water, and sprayed with 70% ethanol.

2.2. Filtering

Water samples were filtered using previously established protocols [43]. Briefly, water samples were thoroughly mixed to suspend any precipitated particulates before an aliquot was measured. The aliquot was first passed through a 20- μm metal sieve (Artesian Systems) before being filtered through a 400-nm-thick SiN Nanomembrane filter (SIM-Pore MSSN400-3L-8.0) in a vacuum filtration set-up (Fig. 2). Each filter was comprised of 3 windows ($0.7 \times 3 \text{ mm}$). In each window, there were 730 slits. Each slit measured $8 \times 50 \mu\text{m}$. This set-up allows for the isolation of an infrequently studied size-fraction (8–20 μm). The design of these membranes paired with applied vacuum allowed large volumes of the collected water samples to be isolated efficiently, with 250 mL taking roughly 15 min to filter. Furthermore, these membranes are optically clear and made of non-plastic biocompatible materials, allowing assays to be performed directly on them. All aliquots filtered were of 250-mL volume. Select filters were stained with Nile red [51] and trypan blue for plastics and cellulosic materials, respectively. After each stain, these filters were rinsed with 2.25 mL. There was no additional processing for filters used for cell culture experiments. Blank filters were run through the aforementioned method as process controls. Prior to filtering, all glassware was scrubbed with soap, rinsed three times with tap water, rinsed three times with DI water, and sprayed with 70% ethanol.

2.3. Imaging

Bright field and fluorescence images of the filtered debris were captured using an epifluorescence microscope. Nile red and trypan blue fluorescence were imaged using the Texas Red (ex. 586 nm/em. 647 nm)

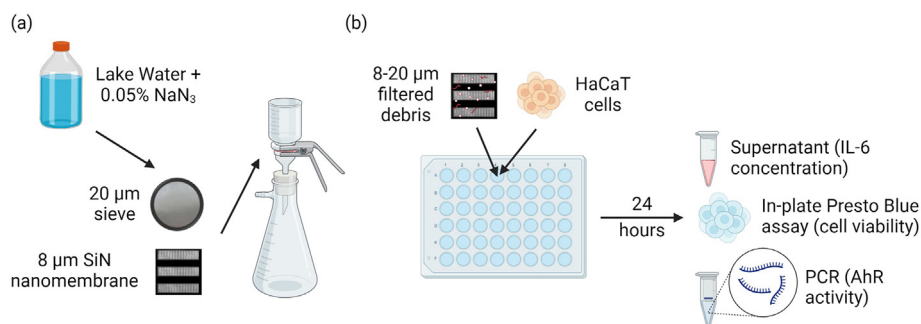


Fig. 2. Experimental set-up. (a) Lake water was collected in 1-L glass bottles and treated with sodium azide before filtering through a 20- μm sieve and an 8- μm SiN nanomembrane. (b) HaCaT cells were exposed to debris for 24 h before cellular components were allocated for various endpoints. Created with [Biorender.com](https://www.biorender.com) under institutional site license, #UU26FRGOHN. HaCaT, immortalized human keratinocyte.

and 4',6-diamidino-2-phenylindole (DAPI, ex. 377 nm/em. 447 nm) filters, respectively. Nile red-positive area was quantified using ImageJ. Briefly, each filter (3 slots per filter) was marked as a region of interest (ROI) using the bright field image. ROIs were then applied to the Nile red image; each ROI was threshold-adjusted, and the percent of pixels above the threshold (percent Nile red) was measured.

2.4. Cell culture

Immortalized human keratinocytes (HaCaTs) were cultured in DMEM supplemented with 10% fetal bovine serum (FBS), and 1% Penicillin Streptomycin and incubated in a humidified incubator at 37 °C with 5% CO₂. Cells were seeded at 1.2×10^5 cells/well on top of SiN nanomembranes placed in 48 well plates. Following 24 h of exposure, supernatant was collected, cell viability was measured in plate, and RNA was isolated.

2.5. Cell viability

After 24 h of exposure, cell culture media was replaced with a 10% presto blue (Invitrogen P50200) solution in the media. Plates were incubated for 30 min at 37 °C before fluorescence was measured (ex. 560 nm/em. 590 nm). Fluorescence values were background-corrected before the percentage of live cells was calculated relative to the media controls. Background control was reagents without cells, and media controls were cells exposed to media only. Blank filters were used to confirm that the results were not due to the SiN nanomembranes.

2.6. AhR activation via real-time reverse transcription quantitative polymerase chain reaction (RT-qPCR)

RNA was isolated using the E.Z.N.A Total RNA Kit I (Omega Bio-Tek R6834) according to the manufacturer's instructions before its concentration was measured using the Nanodrop method. RNA was converted to complementary DNA (cDNA) using the iScript cDNA Synthesis Kit (Bio-Rad 1708890). The resulting cDNA was used to determine the messenger RNA (mRNA) expression of CYP1A1 and CYP1B1 relative to the hypoxanthine phosphoribosyltransferase (HPRT) housekeeping gene and media controls using the PowerUp SYBR Green Master Mix (Applied Biosystems A25742) and the $\Delta\Delta\text{Ct}$ method. HPRT was used as the housekeeping gene, and media controls were cells exposed to media only.

Blank filters were used to confirm that the results were not due to the SiN nanomembranes. Primer sequences for RT-qPCR are listed in [Table 1](#).

2.7. IL-6 Enzyme-linked Immunosorbent Assay (ELISA)

IL-6 concentration was measured in supernatant collected from HaCaTs exposed to filtered debris for 24 h using a human IL-6 uncoated ELISA Kit (Invitrogen 88-7066) in accordance with the manufacturer's instructions. Briefly, on day 1, an ELISA plate (Corning 9018) was coated with a capture antibody and incubated overnight. On day 2, the plate was washed, blocked with diluted ELISA/ELISPOT for 1 h at room temperature, washed again, and 100 μL of IL-6 standard or sample supernatant was added before overnight incubation at 2 °C. The following day (day 3), the plate was washed, incubated with detection antibody for 1 h at room temperature, washed, incubated with streptavidin-horseradish peroxidase (HRP) for 30 min at room temperature, washed, and incubated with tetramethylbenzidine (TMB) for 15 min at room temperature. The reaction was stopped with 0.5 M HCl, and absorbance was measured at 450 nm and 570 nm. Absorbance at 570 nm was used as background correction, and IL-6 sample concentrations were calculated relative to media controls. Media controls were cells exposed to media only. Blank filters were used to confirm that the results were not due to the SiN nanomembranes.

2.8. Statistics

All statistical analyses were performed using GraphPad Prism 10. One-way analyses of variance (ANOVAs) and linear regression tests were performed as needed. Tukey's multiple comparison test was used to determine the significance between exposures following a significant ($p < 0.05$) ANOVA result. An asterisk (*) was used to indicate that the two exposures were significantly different. Exposures were tested with $n = 3$, and each experimental replicate was from a separate 1-L sample collected from LO.

3. Results

3.1. MPs are identified in the filtrate of Lake Ontario samples year-round

Due to the ubiquity of MPs, it is likely they are present in LO, and it is important to assess plastic levels before determining the impacts of

Table 1
Primer sequences [52].

Gene	Forward sequence	Reverse sequence
HPRT	5'-TGCTGAGGATTTGGAAAGGG-3'	5'-ACAGAGGGCTACAATGTGATG-3'
CYP1A1	5'-TAGACACTGATCTGGCTGCAG-3'	5'-GGGAAGGCTCCATCAGCATC-3'
CYP1B1	5'-CATGGCCTTCTCCAGCTTTGT-3'	5'-GGCCACTTCACTGGGTTCATGA-3'

exposure to these particles. To accomplish this, debris from LO water samples between 8 and 20 μm were filtered onto SiN nanomembranes and stained with Nile red and trypan blue. Nile red stains lipophilic particles [51], whereas trypan blue stains cellulosic materials. Composite and Nile red channel images of representative filters are shown in Fig. 3a. All samples filtered contained Nile red-positive particles. The percent Nile red-positive area in the filter windows (3 per filter) was measured using threshold analysis in ImageJ (Fig. 3b and c). Nile red-positive area did not significantly change over time in samples from OBP (Fig. 3b) or between sampling locations in April 2023 (Fig. 3c). However, there was some variation in the amount of debris collected per filter between timepoints and sampling locations (Fig. 3b and c). All samples contained detectable levels of Nile red-positive plastics, although the amount of plastic present in the 8–20 μm range did not vary between samples.

3.2. Filtered debris has no impact on cell viability

Toxicity testing often investigates impacts on mortality at the organism level or viability at the cellular level. A PrestoBlue assay was selected as a proxy for cell viability as it measures alterations in metabolic activity through differences in oxidizable nicotinamide adenine dinucleotide (NADH). HaCaTs were cultured directly on the filtered debris for 24 h before cell viability was assessed. Samples taken at various times from OBP (Fig. 4a) and from various beaches in April 2023 (Fig. 4b) did not exhibit differences in metabolic activity. Overall, none of the filtered samples significantly altered cell viability.

3.3. Debris AhR activity changes over time but not between sampling locations

The AhR has a role in homeostasis, immunity, and cancer, and therefore, exposures that alter AhR activity have implications for human health. CYP1B1 and CYP1A1 mRNA expression were measured via RT-qPCR as a proxy for AhR activation [53] using RNA isolated from HaCaTs cultured on the filtered debris. CYP1B1 expression (Fig. 5) showed statistically significant variation between samples. CYP1A1 expression showed similar trends (Fig. S1). The AhR activity of the filtered debris

varied over time ($p = 0.0104$; Fig. 5a). No spatial variations in AhR activity were observed (Fig. 5b). When AhR activity was plotted as a function of Nile red-positive area, no association was observed ($p = 0.1960$, $r^2 = 0.01021$; Fig. 5c). AhR activity decreased over time but did not change with sampling location.

3.4. Debris IL-6 levels change over time and between sampling locations

Particle exposure often results in inflammation, so MP exposure may induce inflammation as well. IL-6 is a common measure of innate inflammation. The supernatant from HaCaTs exposed to filtered debris was used for an IL-6 ELISA. Elevated IL-6 levels were detected at different times at OBP between November 2021 and November 2023 ($p = 0.0065$; Fig. 6c). Additionally, IL-6 levels were significantly increased relative to blank filters in samples exposed to debris from Hamlin Beach in April 2023 ($p = 0.0008$; Fig. 6a) and OBP in November 2023 ($p = 0.0471$; Fig. 6b). No significant spatial variations were observed between samples collected in April 2023 (Fig. 6b). IL-6 levels were found to have no association with Nile red-positive area ($p = 0.3888$, $r^2 = 0.03395$; Fig. 6c). IL-6 levels varied with time and location sampled.

4. Discussion

Plastic particles were present in all samples and ranged from 0.19% to 0.65% of the filter area (Fig. 3). Percent area was selected over particle enumeration due to the high variability in particle size and the presence of particle agglomeration. Due to the quantification method used, it is difficult to compare concentrations between this study and others. Previous studies have found concentrations of 0.8 particles/L [16] and 30.6 pellets/ m^2 [54]. While these concentrations are likely lower, the sampling methods used differed, and the isolated size fractions were much larger ($>125 \mu\text{m}$ and 63–5,600 μm , respectively). The lack of a trend in plastic amount over time is not wholly unexpected as the area surrounding OBP did not experience any major changes in usage or any spillage events. However, differences between the more urban locations, OBP and DEB, and the more rural beaches, HB and WP, were anticipated based on differences in pollution generated by land and water usage in the surrounding areas. This may be explained by the facts that the two furthest beaches, HB

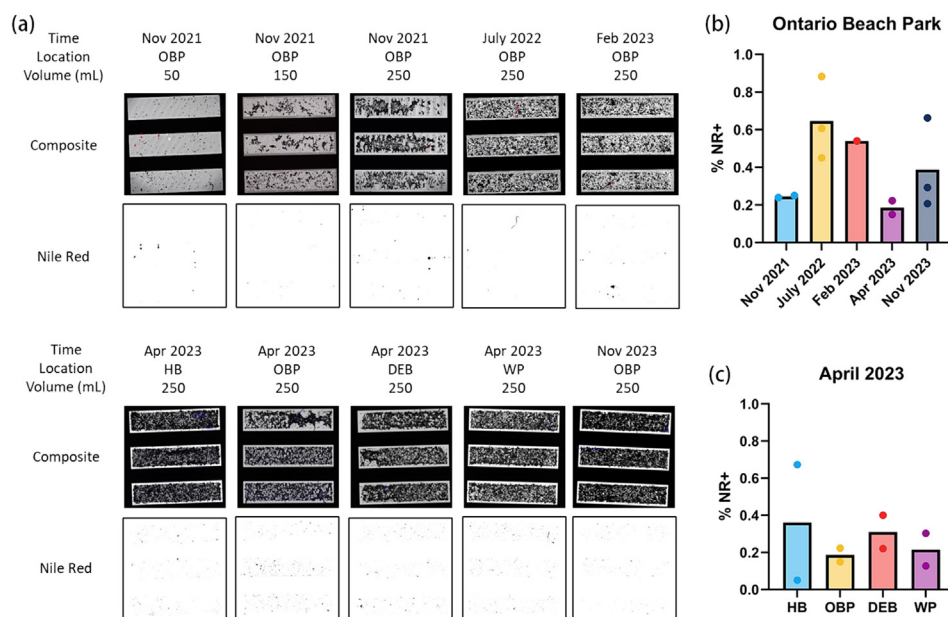


Fig. 3. Lake Ontario debris contains plastic particles. (a) Representative bright field and fluorescence microscopy images of debris isolated from Lake Ontario water samples stained with Nile red (red-top, black-bottom) and trypan blue (blue) and quantification of the percent positive Nile red area per filter to show (b) temporal and (c) spatial trends; $n = 1-3$.

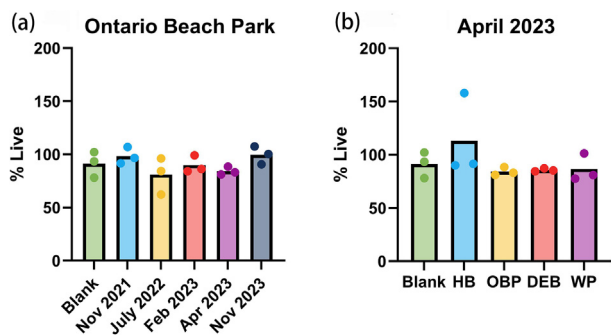


Fig. 4. HaCaTs exposed to filtered debris exhibit no alterations in cell viability. HaCaT cells were exposed to Lake Ontario debris for 24 h. Metabolic activity data are organized to show (a) temporal and (b) spatial trends using samples collected from Ontario Beach Park and in April 2023, respectively. Analyzed by one-way ANOVA followed by Tukey's multiple comparisons test; $n = 3$. ANOVA, analysis of variance; HaCaT, immortalized human keratinocyte.

and WP, are only about 30 miles apart, the nearshore waters of LO near Rochester exhibit strong currents that are largely influenced by wind [55, 56], and models of the Laurentian Great Lakes, of which LO is one, have shown that lake plastic disperses to the sediment and shore [24,57]. It is also of interest to note that the currents [58] and waves [59] along the shore of LO fluctuate between east and west, and thus contaminants can disperse in the near-shore waters in not only the prevailing easterly direction but also westerly directions. Additionally, the lack of observed differences in plastic amount may be due to variations in the size distribution of the plastics present in the different samples that could not be captured since only one size fraction was isolated. On the other hand, variations in the amount of debris collected between samples may be due to samples being collected at different points in the tide cycle and different topographical features between beaches that varied the amount of sediment suspended in the lake during sampling. Overall, samples taken from LO contain plastics, but plastic concentration was not found to vary between samples, pointing to the need to conduct more frequent sampling.

None of the filtered samples induced significant alterations to HaCaT metabolic activity and are therefore assumed not to be cytotoxic (Fig. 4). This may be due to the isolated size fraction being too large to be internalized by the exposed cells [60]. Despite the lack of observed cytotoxicity, the filtered debris still had the potential to impact other components of cellular homeostasis. Studies using pristine plastic particles have observed alterations to cellular activity without impacts on cell viability [61]. Additionally, the lack of cell death following exposure to filtered debris indicates that changes observed in other measured

endpoints are real and not simply an artifact of decreased cell numbers.

AhR activation is of interest as the AhR has roles in cellular homeostasis, immunity, cancer, and development. Since it is a promiscuous receptor with a wide range of ligands, it is frequently used as a xenobiotic sensor. The AhR is a cytosolic receptor that translocates to the nucleus following activation, where select genes are upregulated. Two of the genes that are strongly upregulated following AhR activation in keratinocytes are CYP1B1 and CYP1A1 [62]. The AhR exhibits ligand-specific gene expression [63], so it is not unexpected that significant alterations in expression were observed with CYP1B1 expression (Fig. 5) but not CYP1A1 expression (Fig. S1). Somewhat unexpectedly, AhR activity in the filtered debris depends on the sampling time between November 2021 and November 2023 (Fig. 5a). This may indicate changes to the chemical composition of the pollutants present on the debris and in the water. Similarly, variations in AhR activity between the sampling locations were anticipated due to differences in the rurality of the surrounding locations. Chemical runoff between urban and rural areas does differ [64,65]. Given the wide range of identified AhR ligands, it is plausible that both types of runoffs could exhibit AhR activity in the filtered retentate. However, no AhR activity was observed in April 2023 in samples taken at different locations (Fig. 5b), and a decrease in AhR activity was observed in OBP samples taken between November 2021 and November 2023. Clearly, more sampling is needed to determine if AhR activity is a good biomarker of MP presence and/or lake-water health. Another factor that likely has a role in the AhR activity observed is the fact that the AhR is a cytosolic receptor, and since the filtered debris is likely too large for cellular internalization, AhR activation may go undetected. Similarly, the lack of association between plastic amount and AhR activity (Fig. 5c) is also likely due to variations in the chemical composition of the pollutants present on the debris and in the water due to the vast number and variety of chemicals that act as AhR ligands. Future studies that include analysis of the chemical composition of the filtered debris, in addition to increased sampling frequency, would help investigate this. Additionally, changes in mRNA levels are insufficient on their own to demonstrate receptor activation in the long run; however, following AhR activation by 2,3,7,8-Tetrachlorodibenzo-p-dioxin (TCDD), a common AhR agonist, both CYP1B1 mRNA and protein levels have been shown to increase together [66,67]. To confirm activation, future work will also include an assessment of CYP enzyme activity and protein levels following debris exposure. Exposure to MPs may result in perturbations to AhR signaling through MPs acting as a vector for AhR ligands.

IL-6 is a common marker for general inflammation, which has previously been linked to particle exposure, and MPs are expected to behave similarly to nanoparticles. Although we observed a lack of activity in November 2021, we did observe an increase in IL-6 levels in samples

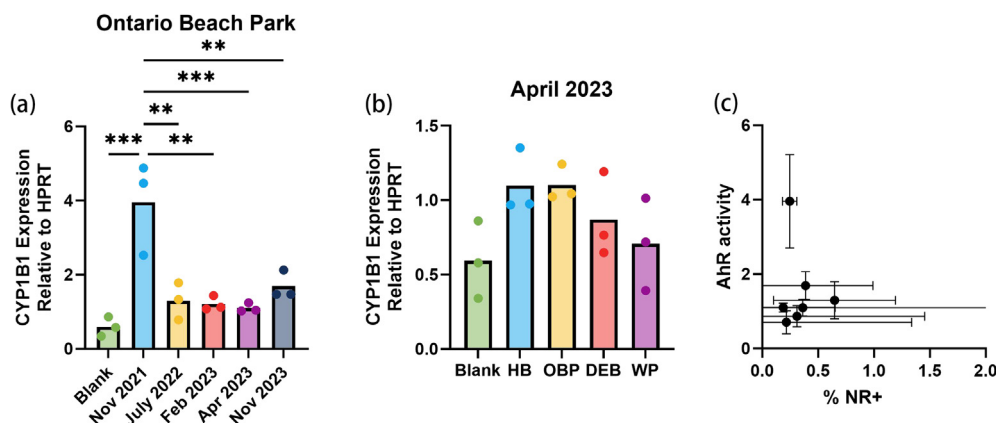


Fig. 5. Exposure to select filtered debris activates the AhR in HaCaT cells. AhR activity was measured through CYP1B1 mRNA levels in HaCaT cells exposed to Lake Ontario debris for 24 h. AhR activity is organized to show (a) temporal and (b) spatial trends using samples collected from Ontario Beach Park and in April 2023, respectively. (c) AhR activity was analyzed as a function of the Nile red-positive area. Analyzed by one-way ANOVA followed by Tukey's multiple comparisons test and/or linear regression; $n = 3$; $***p < 0.001$, $**p < 0.01$. AhR, aryl hydrocarbon receptor.

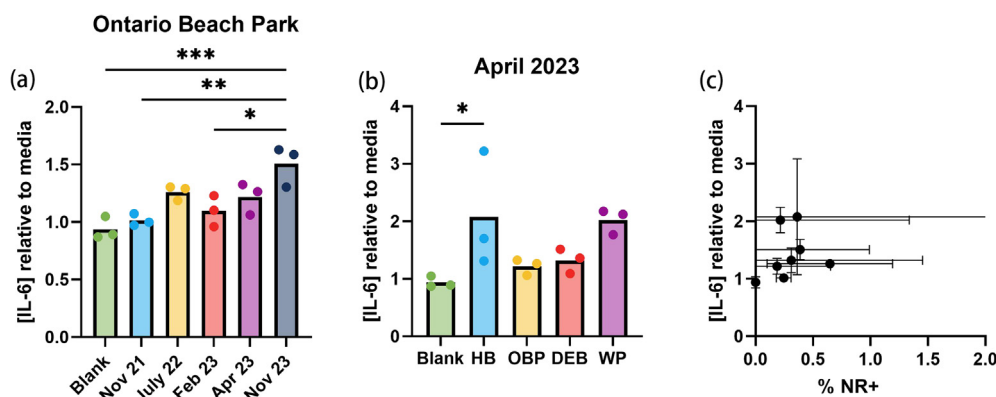


Fig. 6. Exposure to select filtered debris alters IL-6 concentration in HaCaT cells. IL-6 levels were measured by ELISA in supernatant from HaCaT cells exposed to Lake Ontario debris for 24 h. IL-6 levels are organized to show (a) temporal and (b) spatial trends using samples collected from Ontario Beach Park and in April 2023. (c) IL-6 levels were analyzed as a function of the Nile red-positive area. Analyzed by one-way ANOVA followed by Tukey's multiple comparisons test and/or linear regression; $n = 3$; * $p < 0.05$, ** $p < 0.01$, *** $p < 0.001$.

collected at other times, with significantly elevated levels in November 2023 (Fig. 6a). Although not significant, the more rural locations, HB and WP, did have slightly elevated IL-6 levels compared to the more urban locations, OBP and DEB (Fig. 6b). This is likely due to differences in the composition of runoff commonly found between urban and rural locations [24,56], which impact the chemical composition of the pollutants found on the MPs isolated from different locations. Similar to AhR signaling, the lack of association between plastic and IL-6 levels is likely due to differences in the chemical profile of the MPs present (Fig. 6c), although additional sampling is needed to establish an association. The observed alterations in IL-6 levels suggest MP exposure may alter the pro-inflammatory/anti-inflammatory balance.

5. Conclusion

MPs are pervasive and persistent pollutants that humans are inevitably exposed to. Therefore, it is imperative that the risk of exposure to these particles be determined. This study utilized nanomembrane filter technology to investigate the presence and bioactivity of filtered debris containing MPs isolated from the nearshore waters of LO. All samples contained plastics, but the filtered debris did not alter cell viability. Some samples induced significant alterations in AhR activity and/or IL-6 levels. It is important to note that increased CYP1B1 mRNA has been interpreted to indicate AhR activity; however, without protein-level analysis, this cannot be confirmed, and future work should incorporate protein analysis. Temporal trends were observed, but spatial ones were not observed on the specific day the samples were collected. These variations could not be explained by differences in the amount of plastic present, suggesting expanded sampling is needed to fully characterize the impacts of physiochemical and spatiotemporal properties on plastic activity. Importantly, this study demonstrates a novel methodology for isolating and characterizing the bioactivity of debris between 8 and 20 μm , an understudied size fraction, filtered from LO that could be adapted to other waterways. In conclusion, filtered debris from LO contains plastics and is not biologically inert. This preliminary study reports on novel methodology and technology that can be used to analyze additional water samples and highlights the need for increased sampling to determine any seasonal and temporal effects. Ultimately, the results of this study and future applications of this methodology will aid in understanding the hazard and risk MP exposure poses to humans.

CRedit authorship contribution statement

S.M.: methodology, investigation, writing - original draft, writing - review & editing, visualization. L.D.: conceptualization, writing - review & editing, funding acquisition, supervision.

Declaration of competing interest

The authors declare that they have no known conflicts of interest.

Acknowledgments

We thank Dr. Samantha Romanick, PhD (University of Rochester) for sharing her knowledge on filtering using SiN nanomembranes and Dr. James McGrath, PhD (University of Rochester) for the use of his laboratory space for filtering experiments. This work was supported by the National Institute of Environmental Health Sciences (NIEHS R01 ES021492), the University of Rochester Toxicology Training Program (NIEHS T32 ES007026), and the University of Rochester Environmental Health Sciences Center (NIEHS P30 ES001247).

Appendix A. Supplementary data

Supplementary data to this article can be found online at <https://doi.org/10.1016/j.eehl.2024.05.004>.

References

- [1] International Union for Conservation of Nature, Marine plastic pollution. <https://www.iucn.org/resources/issues-brief/marine-plastic-pollution>. (Accessed 17 August 2023).
- [2] R.C. Thompson, Y. Olsen, R.P. Mitchell, A. Davis, S.J. Rowland, A.W.G. John, D. McGonigle, A.E. Russell, Lost at sea: where is all the plastic? *Science* 304 (2004) 838, <https://doi.org/10.1126/science.1094559>.
- [3] C.J. Moore, Synthetic polymers in the marine environment: a rapidly increasing, long-term threat, *Environ. Res.* 108 (2008) 131–139, <https://doi.org/10.1016/j.envres.2008.07.025>.
- [4] E.S. Germanov, A.D. Marshall, L. Bejder, M.C. Fossi, N.R. Loneragan, Microplastics: no small problem for filter-feeding megafauna, *Trends Ecol. Evol.* 33 (2018) 227–232, <https://doi.org/10.1016/j.tree.2018.01.005>.
- [5] A. Andrady, Microplastics in the marine environment, *Mar. Pollut. Bull.* 62 (2011) 1596–1605, <https://doi.org/10.1016/j.marpolbul.2011.05.030>.
- [6] Y.K. Song, S.H. Hong, M. Jang, G.M. Han, S.W. Jung, W.J. Shim, Combined effects of UV exposure duration and mechanical abrasion on microplastic fragmentation by polymer type, *Environ. Sci. Technol.* 51 (2017) 4368–4376, <https://doi.org/10.1021/acs.est.6b06155>.
- [7] J. Gigault, B. Pedrono, B. Maxit, A.T. Halle, Marine plastic litter: the unanalyzed nano-fraction, *Environ. Sci. Nano* 3 (2016) 346–350, <https://doi.org/10.1039/C6EN00088H>.
- [8] A. Ter Halle, L. Jeanneau, M. Martignac, E. Jardé, B. Pedrono, L. Brach, J. Gigault, Nanoplastic in the North Atlantic subtropical gyre, *Environ. Sci. Technol.* 51 (2017) 13689–13697, <https://doi.org/10.1021/acs.est.7b03667>.
- [9] A. Turner, R. Arnold, T. Williams, Weathering and persistence of plastic in the marine environment: lessons from LEGO, *Environ. Pollut.* 262 (2020) 114299, <https://doi.org/10.1016/j.envpol.2020.114299>.
- [10] D.K.A. Barnes, F. Galgani, R.C. Thompson, M. Barlaz, Accumulation and fragmentation of plastic debris in global environments, *Philos. Trans. R. Soc. B Biol. Sci.* 364 (2009) 1985–1998, <https://doi.org/10.1098/rstb.2008.0205>.

- Chemosphere 221 (2019) 333–341, <https://doi.org/10.1016/j.chemosphere.2019.01.056>.
- [62] H.I. Swanson, Cytochrome P450 expression in human keratinocytes: an aryl hydrocarbon receptor perspective, *Chem. Biol. Interact.* 149 (2004) 69–79, <https://doi.org/10.1016/j.cbi.2004.08.006>.
- [63] S. Safe, H. Han, J. Goldsby, K. Mohankumar, R.S. Chapkin, Aryl hydrocarbon receptor (AhR) ligands as selective AhR modulators: genomic studies, *Curr. Opin. Toxicol.* 11–12 (2018) 10–20, <https://doi.org/10.1016/j.cotox.2018.11.005>.
- [64] M.A. Mallin, V.L. Johnson, S.H. Ensign, Comparative impacts of stormwater runoff on water quality of an urban, a suburban, and a rural stream, *Environ. Monit. Assess.* 159 (2009) 475–491, <https://doi.org/10.1007/s10661-008-0644-4>.
- [65] O. Al-Mashaqbeh, A. Jiries, Z. El-HajAli, Stormwater runoff quality generated from an urban and a rural area in the Amman-Zarqa basin, *WIT Trans. Ecol. Environ.* 182 (2014) 379–390, <https://doi.org/10.2495/WP140331>.
- [66] A. Jacob, A.M. Hartz, S. Potin, X. Coumoul, S. Yousif, J.-M. Scherrmann, B. Bauer, X. Declèves, Aryl hydrocarbon receptor-dependent upregulation of Cyp1b1 by TCDD and diesel exhaust particles in rat brain microvessels, *Fluids Barriers CNS* 8 (2011) 23, <https://doi.org/10.1186/2045-8118-8-23>.
- [67] J. Procházková, A. Kozubík, M. Machala, J. Vondráček, Differential effects of indirubin and 2,3,7,8-tetrachlorodibenzo-*p*-dioxin on the aryl hydrocarbon receptor (AhR) signalling in liver progenitor cells, *Toxicology* 279 (2011) 146–154, <https://doi.org/10.1016/j.tox.2010.10.003>.